

Crystal Structure, Solubility, and Mutarotation of the Rare Monosaccharide D-Psicose

Kazuhiro Fukada,*[1] Tomohiko Ishii,[2] Katsushi Tanaka,[2] Masatsugu Yamaji,[2] Yuya Yamaoka,[2] Ken-ichi Kobashi,[2] and Ken Izumori[3]

[1]Department of Applied Biological Science, Faculty of Agriculture, Kagawa University, 2393 Ikenobe, Kagawa 761-0795

[2]Department of Advanced Materials Science, Faculty of Engineering, Kagawa University, Takamatsu 761-0396

[3]Rare Sugar Research Center, Kagawa University, 2393 Ikenobe, Kagawa 761-0795

Received May 27, 2010; E-mail: fukada@ag.kagawa-u.ac.jp

X-ray crystal analysis for D-psicose (C3-position epimer of D-fructose) crystallized from aqueous solution was successfully performed for the first time. It was confirmed that D-psicose crystallized solely as β-D-pyranose with 1C ($^1C_4$ (D)) conformation. The crystal system (orthorhombic), space group (#19, $P2_12_12_1$), and number of molecules per unit cell ($Z = 4$) are the same as those for β-D-fructopyranose, α-L-sorbopyranose, and α-D-tagatopyranose. Solubility of D-psicose at 25 °C was 291 g per 100 g water. Mutarotation was further investigated recording the time course of specific rotation [α] at 589 nm after the dissolution of D-psicose in water. It is thought that [α] for β-D-psicopyranose in water may be ca. $-85\,\mathrm{deg\,dm^{-1}\,g^{-1}\,cm^3}$. The time course of absorbance at 280 nm after the dissolution of D-psicose was also measured to see the development of open-chain carbonyl-form in the solution, and the first-order kinetic behavior with the rate constant $k = 4.44\,\mathrm{ms^{-1}}$ was confirmed. Assuming the equilibrium content of carbonyl-form of D-psicose as 0.2%, the molar absorption coefficient, ε, for the carbonyl-form was estimated to be $160\,\mathrm{cm^{-1}\,M^{-1}}$.

Recent biotechnological advances have dramatically increased the possibility of producing rare monosaccharides in an environmentally friendly way. Izumoring is a biotechnological strategy, which allows the green production of any of the isomeric hexoses, pentoses, and tetroses.[1–3] In Izumoring, epimerization of ketoses at the C3 position is one of the key processes for the syntheses of various monosaccharides. D-Tagatose 3-epimerase (D-TE) is employed as a versatile catalyst for the C3 epimerization of all ketohexoses and ketopentoses. A catalytic mechanism of D-TE has been proposed, based on X-ray crystal analysis for the complexes of D-TE and D-tagatose/D-fructose.[4] In this study we utilized immobilized D-TE to produce a rare monosaccharide D-psicose (Psi) from inexpensive D-fructose (Fru) (Figure 1).

It has recently been demonstrated that Psi has interesting functional properties; for example, Psi could be useful in preventing postprandial hyperglycemia in diabetic patients[5] and be a potential anthelmintic.[6] It is further expected that Psi may be used as a sweetener for functional foods with high antioxidant activity and low calorie content.[7]

It should be stressed that Psi had only existed as a syrup,[8] and no crystalline sample had been made until recently. Through the success of large-scale production of highly pure Psi by the epimerization of Fru with the aid of D-TE, however, crystallization of Psi was finally achieved and single crystals of Psi suitable for X-ray diffraction analysis have recently been obtained. The present work reports the single crystal structure of Psi to complete the data set of crystal structures of ketohexoses.[9–13] Besides the crystal structure, the aqueous solubility and mutarotation of Psi were also investigated using the crystalline sample. These solution properties are important for carbohydrate science as well as for quality control in large-scale Psi production.

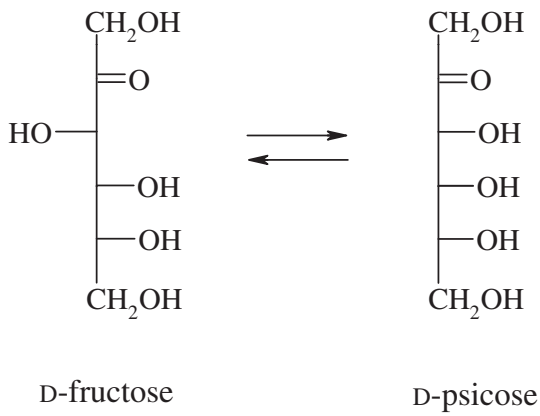

Figure 1. Conversion of D-fructose (Fru) to D-psicose (Psi) by D-tagatose 3-epimerase. The equilibrium molar ratio is 3 (Fru) to 1 (Psi) at 25 °C.

Experimental

Materials. Psi was obtained by the epimerization of Fru using immobilized D-TE with the equilibrium molar ratio 1 versus 3.[14,15] To remove Fru from the mixed sugar solution, column chromatography was performed using a Dowex 50W-X2 (Ca^{2+}-form) or Hitachi GL-C611, and the fractions

Published on the web September 25, 2010; doi:10.1246/bcsj.20100148

containing Psi was concentrated up to ca. 80 wt % by a rotary evaporator at 40 °C. Crystallization of Psi succeeded at room temperature within 2–3 days. The melting point of Psi was confirmed to be 96 °C by means of differential scanning calorimetry (Rigaku DSC 8240D).

X-ray Diffraction Analysis. The X-ray diffraction study was performed with a colorless block crystal ($0.20 \times 0.20 \times 0.20\,mm^3$) using a Rigaku AFC7S diffractometer with graphite monochromated Mo Kα radiation. The crystal structure was solved by the direct methods SIR92[16] and expanded using Fourier techniques.[17] Non-hydrogen atoms were refined anisotropically and hydrogen atoms were refined using the riding model. The final cycle of full-matrix least-squares refinement[18] on F was based on 1105 observed reflections ($I > 3.00\sigma(I)$) with the empirical absorption corrections, and 122 variable parameters converged (largest parameter shift was 0.00 times its esd) with unweighted (weighted) agreement factor; $R_1 = 0.043$ ($wR_2 = 0.044$).

Crystallographic data have been deposited with Cambridge Crystallographic Data Centre: Deposition number CCDC-776516. Copies of the data can be obtained free of charge via http://www.ccdc.cam.ac.uk/conts/retrieving.html (or from the Cambridge Crystallographic Data Centre, 12, Union Road, Cambridge, CB2 1EZ, U.K.; Fax: +44 1223 336033; e-mail: deposit@ccdc.cam.ac.uk).

Solubility. To estimate solubility of Psi in the temperature range 0 to 50 °C, Psi crystal was finely smashed, mixed with pure water in a glass vial, and stored in a thermostat water bath (Lauda RMS6) with occasional stirring for at least five days. After the dissolution equilibrium was attained, Psi content in supernatant, which corresponded to aqueous solubility, was estimated by means of densitometry based on the predetermined calibration curve for the relation between Psi content and solution density. For the accurate density measurements of aqueous Psi, an oscillating tube density meter (Anton Paar DMA5000, Gratz) was employed. The thermostat water bath was then set at a higher temperature and new dissolution equilibrium was attained within another five days.

Mutarotation. The time course of the optical rotation at 589 nm (Na D-line) for the Psi solution was monitored after the dissolution of the sugar powder in water employing a digital spectropolarimeter (Jasco P-1010, Tokyo). Psi crystals were finely crushed for prompt dissolution (within 10 s), and the solution was introduced into a 1-dm path length quartz cell equipped with circulating water jacket for temperature controlling. Measurements were performed at 15, 25, 35, and 45 °C. The absorbance at 280 nm was also monitored employing an UV-VIS spectrometer (Hitachi U-1800, Tokyo) with a 1-cm path length quartz cell at 25 °C to see the development of the open-chain carbonyl-form after dissolution.

Results and Discussion

Molecular Geometry. Crystallographic data and refinement parameters of the X-ray analysis are presented in Table 1. The perspective view of the Psi molecule obtained from the X-ray analysis is illustrated in Figure 2 and bond lengths and bond angles for non-hydrogen atoms are summarized in Table 2. Although Psi in aqueous solution consists of five tautomers, α-furanose, β-furanose, α-pyranose, β-pyranose,

Table 1. Crystallographic and Refinement Data for β-D-Psicopyranose

Formula	$C_6H_{12}O_6$
Formula weight	180.16
Crystal system	Orthorhombic
Space group	$P2_12_12_1$ (#19)
T/°C	25
Wavelength/Å	0.71069
μ(Mo Kα)/cm^{-1}	1.44
a/Å	8.693(2)
b/Å	11.185(4)
c/Å	7.745(2)
V/Å^3	753.1(3)
Z	4
Calculated density/g cm^{-3}	1.589
Reflections collected	6914
Independent reflections ($R_{int} = 0.080$)	1236
Observed reflections ($I > 3\sigma(I)$)	1105
R_1 (observed data) $= \Sigma(\|F_{obs}\| - \|F_{calc}\|)/\Sigma\|F_{obs}\|$	0.043
$wR_2 = [\Sigma w(\|F_{obs}\| - \|F_{calc}\|)^2/\Sigma wF_{obs}^2]^{1/2}$	0.044

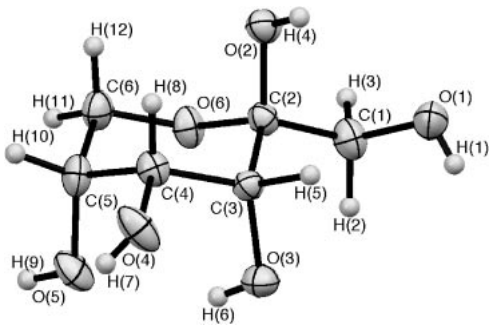

Figure 2. Molecular structure and atom labeling of β-D-psicopyranose in single crystal.

Table 2. Geometric Parameters for Non-Hydrogen Atoms in β-D-Psicopyranose

Bond length			Bond angle			
Atom	Atom	Distance /Å	Atom	Atom	Atom	Angle /degree
O(1)	C(1)	1.433(4)	O(1)	C(1)	C(2)	109.1(2)
O(2)	C(2)	1.411(3)	O(2)	C(2)	O(6)	107.3(2)
O(3)	C(3)	1.432(3)	O(2)	C(2)	C(1)	110.8(2)
O(4)	C(4)	1.424(4)	O(2)	C(2)	C(3)	109.5(2)
O(5)	C(5)	1.426(4)	O(3)	C(3)	C(2)	111.2(2)
O(6)	C(2)	1.423(4)	O(3)	C(3)	C(4)	112.0(2)
O(6)	C(6)	1.435(4)	O(4)	C(4)	C(3)	110.4(2)
C(1)	C(2)	1.517(4)	O(4)	C(4)	C(5)	113.0(2)
C(2)	C(3)	1.542(4)	O(5)	C(5)	C(4)	106.4(2)
C(3)	C(4)	1.519(4)	O(5)	C(5)	C(6)	112.5(2)
C(4)	C(5)	1.517(4)	O(6)	C(2)	C(1)	104.6(2)
C(5)	C(6)	1.511(4)	O(6)	C(2)	C(3)	110.1(2)
			C(6)	O(6)	C(2)	115.3(2)
			O(6)	C(6)	C(5)	111.1(2)
			C(1)	C(2)	C(3)	114.2(2)
			C(2)	C(3)	C(4)	109.6(2)
			C(3)	C(4)	C(5)	111.3(2)
			C(4)	C(5)	C(6)	109.6(3)

Table 3. Summary of Single Crystal Structure of Ketohexoses

Sugar	Ring structure	Orientation of OH groups				Unit cell volume/Å^3	Reference
		C2	C3	C4	C5		
D-Psicose	β-Pyranose (1C)	axial	axial	equatorial	axial	753.1	this work
D-Fructose	β-Pyranose (1C)	axial	equatorial	equatorial	axial	747.0	10, 11
L-Sorbose	α-Pyranose (1C)	axial	equatorial	equatorial	equatorial	745.9	13
D-Tagatose	α-Pyranose (C1)	axial	axial	equatorial	equatorial	722.8	12

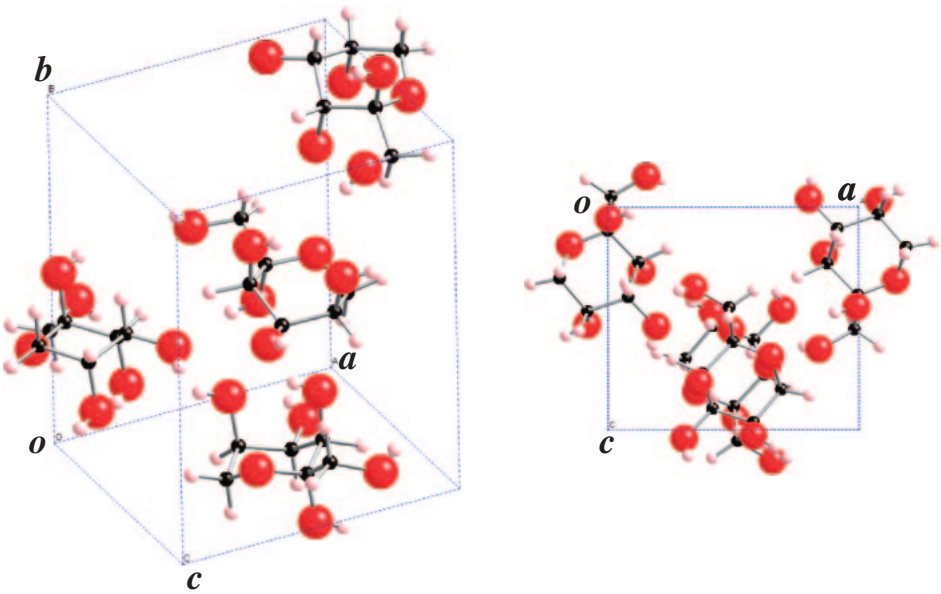

Figure 3. Molecular packing of β-D-psicopyranose in the unit cell (left) and the projected image along the b axis on the a–c plane (right).

and carbonyl-form, Psi crystallized solely as β-D-pyranose with 1C ($^1C_4$ (D)) conformation. Figure 2 shows the six-membered pyranose ring with three axial OH groups at C2-, C3-, and C5-positions and one equatorial OH at C4-position. As had been suggested with α-ribopyranose,[9] the ring conformation is stabilized by intramolecular hydrogen bonding between O(3)H and O(5). The distance between O(3)···O(5) and H(6)···O(5) is 2.719 and 2.035 Å, respectively. The crystal system (orthorhombic), space group (#19, $P2_12_12_1$), and number of molecules per unit cell ($Z = 4$) are the same as those for β-D-fructopyranose, α-L-sorbopyranose, and α-D-tagatopyranose. In Table 3, molecular conformation of the four ketohexoses in the crystal is summarized.

The molecular packing of Psi in the unit cell and the projected image along the b axis on the a–c plane is shown in Figure 3. One can see that the pyranose ring planes are almost parallel to the a–c plane as reported for β-D-fructopyranose. The lattice parameters of Psi are close to those of β-D-fructopyranose ($a = 8.088$, $b = 9.204$, $c = 10.034$ Å, $V = 746.95$ Å^3), but the b axis for Psi is slightly longer (Table 1). Steric hindrance by the axial OH at C3-position is a possible cause for the elongation of the b axis.

From the measurements of the X-ray crystal orientation using a rod-shaped crystal of Psi, it was confirmed that the b axis was almost in parallel with the longitudinal direction of the crystal. The indexes of the crystal side planes were (101) and ($\bar{1}01$), or ($10\bar{1}$) and ($\bar{1}0\bar{1}$), respectively. The end of the crystal was cracked and the resulting prism-shape had indexes of (120) and ($\bar{1}\bar{2}0$), respectively.

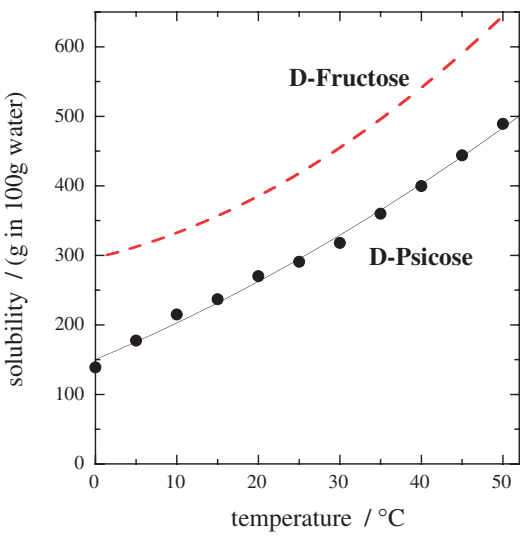

Figure 4. Solubility of D-psicose in water as a function of temperature. Literature data of aqueous solubility for anhydrous D-fructose is indicated by the broken line.

Aqueous Solubility. Figure 4 shows the temperature dependence of the aqueous solubility of Psi and the literature data for the solubility of Fru.[19] It can be seen that Psi is highly

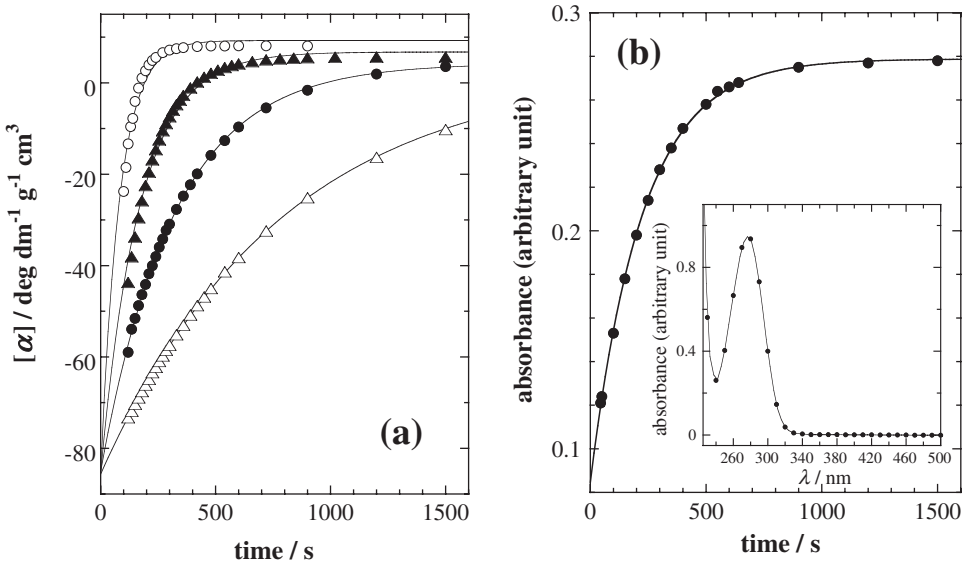

Figure 5. Time course of optical rotation at 589 nm (a) and absorbance at 280 nm (b) after dissolution of D-psicose in water (10 wt %). Temperature is 15 (△), 25 (●), 35 (▲), and 45 °C (○), respectively. Nonlinear least-squares fitting parameters for (a) are summarized in Table 4 and for (b): $\mathrm{abs}(t) = 0.28\text{–}0.19 \cdot \exp(-4.44 \times 10^{-3}\,\mathrm{s^{-1}} \cdot t)$. Inset in (b) is the UV spectrum for aqueous solution of D-psicose (30 wt %).

Table 4. Nonlinear Least-Squares Fitting Parameters for the Time Course of $[\alpha]$ after Dissolution of Psi in Water; $[\alpha](t) = [\alpha]_\infty + ([\alpha]_0 - [\alpha]_\infty)\exp(-k \cdot t)$[a)]

Temperature/°C	k/ms^{-1}	$[\alpha]_\infty$/deg dm^{-1} g^{-1} cm^3
15	1.27	3.4
25	3.12	4.6
35	5.92	5.7
45	12.2	8.1

a) $[\alpha]_0$ was estimated to be -85 deg dm^{-1} g^{-1} cm^3.

soluble in water; at 25 °C (50 °C), 291 g (489 g) of Psi can be dissolved in 100 g water to give a 74 wt % (83 wt %) solution with density of 1.35 g cm^{-3}. This graph provides us the basic information for the recrystallization recipe of Psi from aqueous solution. Solubility of the anhydrous crystal of Fru is higher than Psi as shown in Figure 4. It is known that the dihydrate of Fru can be formed below 20 °C, which is supposed to be Fru's thermodynamically stable state.[19] At the present stage, no hydrated crystal of Psi has been confirmed.

Mutarotation. Finally we investigated mutarotation recording the time course of specific rotation $[\alpha]$ at 589 nm after the dissolution of D-psicose in water (10 wt %). To our best knowledge, mutarotation of Psi has not been reported so far. Figure 5a shows the time course of $[\alpha]$ at various temperatures and the nonlinear least-squares fitting curves by single-exponential equations (Table 4). When temperature was elevated, significant acceleration of mutarotation and an increase of the equilibrium value of specific rotation, $[\alpha]_\infty$, were confirmed while the initial value, $[\alpha]_0$, did not change with temperature. These results suggest β-D-psicopyranose in crystal first dissolves in water without configuration change and then equilibrates gradually to a mixture of tautomers at a temperature dependent rate constant. The equilibrium ratio of tautomers is also temperature dependent. It is thought that $[\alpha]$ for β-D-psicopyranose in water may be ca. -85 deg dm^{-1} g^{-1} cm^3. However, caution is necessary for this evaluation of $[\alpha]$ since the α- and β-configurations for a reducing sugar frequently coexist in the same crystal structure and X-ray diffraction analysis cannot accurately detect components that make up less than 10% of the crystal.[9]

It is interesting to show the time course of absorbance at 280 nm after dissolution of D-psicose (Figure 5b) since the absorbance at this wavelength can only be attributed to open-chain carbonyl-form in the five tautomers. The data points in Figure 5b were well fitted by a single-exponential equation having a rate constant, 4.44 ms^{-1}, which was faster than that for mutarotation at 25 °C (3.12 ms^{-1}). Figure 6 illustrates the multiple equilibria between the five tautomers of Psi in solution. The kinetic behavior for the concentration of chain-form, [chain], can be described by the following equation;

$$[\mathrm{chain}] = [\mathrm{chain}]_\infty + ([\mathrm{chain}]_0 - [\mathrm{chain}]_\infty)\exp[-(k_+ + k_-)t] \quad (1)$$

where subscript ∞ and 0 represent equilibrium and initial values, respectively, $k_+ = k_1 + k_2 + k_3 + k_4$, and $k_- = k_{-1} + k_{-2} + k_{-3} + k_{-4}$. Referring to the fitting parameters in Figure 5b, $k_+ + k_-$ should be 4.44 ms^{-1}at 25 °C. Interpretation of the rate constant for mutarotation, on the other hand, is not as simple as UV absorbance kinetics since all five tautomers contribute to the specific rotation and the molecular rotatory power of each tautomer is not yet known. Note that the fitting curve in Figure 5b started from 0.09 at $t = 0$ suggesting a contamination with the absorbance at this wavelength in the crystal. Subtracting the absorption by the contamination and assuming the equilibrium content of the carbonyl-form at 25 °C as 0.2%,[20] the molar absorption coefficient at $\lambda_{\max} = 280$ nm, ε, for the open-chain carbonyl-form of Psi was estimated to be 160 cm^{-1} M^{-1}, which was approximately ten (eight) times larger than that of ε for aqueous acetone with $\lambda_{\max} = 265$ nm

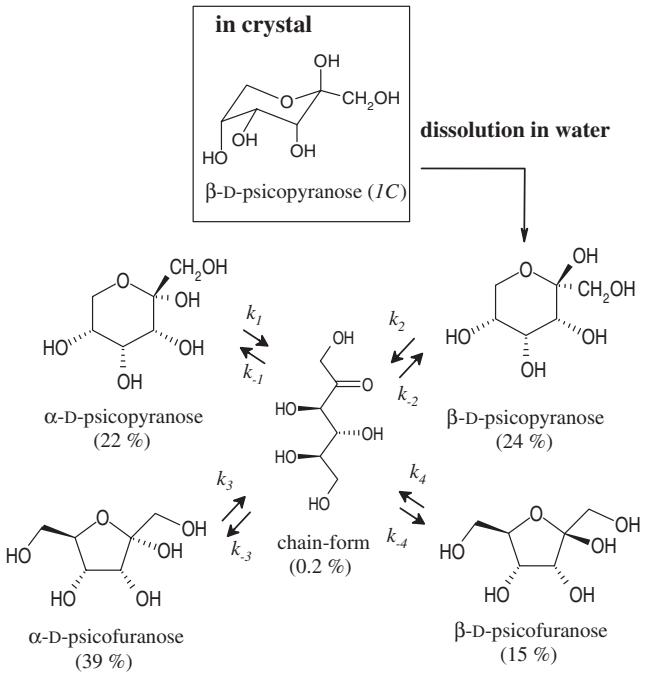

Figure 6. Illustration for molecular structures of D-psicose in crystal and in aqueous solution. Equilibrium contents of each tautomer at 27 °C are indicated according to the literature.[20]

(1,3-dihydroxy-2-propanone with $\lambda_{max} = 270$ nm).[21] The observed increase of extinction coefficient and the red-shift for the $n \rightarrow \pi^*$ transition of C=O group may be attributed to the more extensive π^* molecular orbital in the open-chain Psi molecule compared to acetone.

This work was financially supported by the CITY AREA program by the Ministry of Education, Culture, Sports, Science and Technology of Japan (MEXT).

References

1 K. Izumori, *Naturwissenschaften* **2002**, *89*, 120.
2 T. B. Granström, G. Takata, M. Tokuda, K. Izumori, *J. Biosci. Bioeng.* **2004**, *97*, 89.
3 K. Izumori, *J. Biotechnol.* **2006**, *124*, 717.
4 H. Yoshida, M. Yamada, T. Nishitani, G. Takada, K. Izumori, S. Kamitori, *J. Mol. Biol.* **2007**, *374*, 443.
5 T. Matsuo, K. Izumori, *Biosci. Biotechnol. Biochem.* **2006**, *70*, 2081.
6 M. Sato, H. Kurose, T. Yamasaki, K. Izumori, *J. Nat. Med.* **2008**, *62*, 244.
7 Y. Sun, S. Hayakawa, M. Ogawa, K. Fukada, K. Izumori, *J. Agric. Food Chem.* **2008**, *56*, 4789.
8 *Data Book of Biochemistry I*, ed. by The Japanese Biochemical Society, Tokyo-Kagaku-Dohjin, Tokyo, **1979**, p. 427.
9 G. A. Jeffrey, W. Saenger, *Hydrogen Bonding in Biological Structures*, Springer, Berlin, **1991**, Chap. 13.
10 J. A. Kanters, G. Roelofsen, B. P. Alblas, I. Meinders, *Acta Crystallogr., Sect. B* **1977**, *33*, 665.
11 S. Takagi, G. A. Jeffrey, *Acta Crystallogr., Sect. B* **1977**, *33*, 3510.
12 S. Takagi, R. D. Rosenstein, *Carbohydr. Res.* **1969**, *11*, 156.
13 S. H. Kim, R. D. Rosenstein, *Acta Crystallogr.* **1967**, *22*, 648.
14 H. Itoh, T. Sato, K. Izumori, *J. Ferment. Bioeng.* **1995**, *80*, 101.
15 K. Takeshita, A. Suga, G. Takada, K. Izumori, *J. Biosci. Bioeng.* **2000**, *90*, 453.
16 A. Altomare, G. Cascarano, C. Giacovazzo, A. Guagliardi, M. C. Burla, G. Polidori, M. Camalli, *J. Appl. Cryst.* **1994**, *27*, 435.
17 P. T. Beurskens, G. Admiraal, G. Beurskens, W. P. Bosman, R. de Gelder, R. Israel, J. M. M. Smits, *The DIRDIF-99 Program System, Technical Report of the Crystallography Laboratory*, University of Nijmegen, The Netherlands, **1999**.
18 Least-squares function minimized: $\Sigma w(|F_{obs}| - |F_{calc}|)^2$ where w is the least-squares weight.
19 F. E. Young, F. T. Jonses, H. J. Lewis, *J. Phys. Chem.* **1952**, *56*, 1093.
20 R. N. Goldberg, Y. B. Tewari, *J. Phys. Chem. Ref. Data* **1989**, *18*, 809.
21 G. Avigad, S. Englard, I. Listowsky, *Carbohydr. Res.* **1970**, *14*, 365.